International Journal of Systems Science
volume 34, number 3, 20 February 2003, pages 167–179

B. Subudhi is presently with NIT-Rourkela, India
bidyadhar@nitrkl.ac.in, bidya2k@yahoo.com

Singular perturbation approach to trajectory tracking of flexible robot with joint elasticity

B. Subudhi and A. S. Morris*

The control problem of a robot manipulator with flexures both in the links and joints was investigated using the singular perturbation technique. Owing to the combined effects of the link and joint flexibilities, the dynamics of this type of manipulator become more complex and under-actuated leading to a challenging control task. The singular perturbation being a successful technique for solving control problems with under-actuation was exploited to obtain simpler subsystems with two-time-scale separation, thus enabling easier design of subcontrollers. Furthermore, simultaneous tracking and suppression of vibration of the link and joint of the manipulator is possible by application of the composite controller, i.e. the superposition of both subcontrol actions. In the first instance, the design of a composite controller was based on a computed torque control for slow dynamics and linear-quadratic fast control. Later, to obtain an improved control performance under model uncertainty, the composite control action was achieved using the radial basis function neural network for the slow control and a linear-quadratic fast control. It was confirmed through numerical simulations that the proposed singular perturbation controllers suppress the joint and link vibrations of the manipulator satisfactorily while a perfect trajectory tracking was achieved.

1. Introduction

Robot manipulators constructed with lightweight arms offer a number of potential advantages including higher payload-to-arm weight ratio, higher speed and larger work space compared with their rigid counterparts, which make them indispensable for many specialized applications, namely space craft and teleportation, etc. However, due to distributed link flexibility such manipulators pose much more control complexity. Besides the link flexure, there exists a significant amount of joint flexure in lightweight manipulators that comes from the drive mechanism (Spong 1987). If both these flexures are considered then the resulting dynamics of the manipulator becomes more complex and the control complexities are further compounded.

Received 16 January 2001. Revised 27 February 2003. Accepted 16 April 2003.

Department of Automatic Control and Systems Engineering, University of Sheffield, Sheffield S1 3JD, UK.
* To whom correspondence should be addressed.
e-mail: a.morris@sheffield.ac.uk

Various modelling techniques have been proposed in the literature to investigate the dynamic characteristic of flexible manipulators, such as the Lagrangian–Euler assumed modes method (Geniele *et al.* 1997), the finite element approach (Usoro *et al.* 1986, Bayo 1987), and Kane's approach (Everett 1989). However, most modelling approaches consider either only link flexibility (Usoro *et al.* 1986, Geniele *et al.* 1997) or only joint flexibility (Spong 1987, 1989, Ge 1996), probably to avoid complexity in the dynamic equations. The compliance of the manipulators due to links and joints becomes a significant factor that affects the precision of the manipulators when they are expected to move at high speeds. Studies on dynamic simulations of one- and two-link robot manipulators with both link and joint flexibility (Yang and Donath 1988, Yuan and Lin 1991) have revealed that the joint flexibility as well as the link flexibility needs to be considered in the analysis and control of such manipulator systems. In this work, both link flexibility and joint flexibility are considered. Link flexibility is modelled using the assumed modes of vibration model (Meirovitch 1986) and joint flexibility is modelled as a linear torsional spring model

International Journal of Systems Science ISSN 0020–7721 print/ISSN 1464–5319 online © 2003 Taylor & Francis Ltd
http://www.tandf.co.uk/journals
DOI: 10.1080/0020772031000135450

(Spong 1987). The dynamics of a single-link flexible manipulator with elastic joint has been derived using the Langrange's equation. The resulting dynamic model obtained is a distributed parameter system involving partial differential equations. Therefore, designing control schemes for this system becomes difficult because the discretization of the partial differential equations gives rise to dynamical systems of very high order. The resulting large size of the system model also causes problems when it is necessary to simulate the system model on-line. Another difficulty encountered in controlling flexible link manipulators is because they have fewer available control inputs compared with the degrees of freedom, i.e. all modes of flexure in each link and the angular position of the link have to be controlled simultaneously by adjusting a single actuating torque. This difficulty is accentuated in the case where both the links and joints are flexible since the actuating torque for each link then has to control the flexure of both the link and its corresponding joint. In the past, the problem of controlling under-actuated systems has been resolved successfully by suitable application of the singular perturbation technique that uses a perturbation parameter to divide the complex dynamic systems into simpler subsystems at different time scales (Kokotovic 1984). Therefore, the task of designing controllers for individual subsystems becomes easy, and this has motivated applications to many engineering systems such as large-scale power systems, space structures, and aircraft and rocket systems (Saksena *et al.* 1984). Furthermore, this technique has been exploited, first by Siciliano and Book (1988) for trajectory control of a single-link flexible manipulator, and later extended to a multilink flexible manipulator (Siciliano *et al.* 1992, Aoustin and Chevallereau 1993). Aoustin *et al.* (1994) compared the performances of different control schemes, namely sliding mode control, proportional and derivative control, linear-quadratic regulator (LQR) and feedback linearization control on an experimental single-flexible link. Their investigation showed that the singular perturbation-based control design is simple, computationally less intensive and gives the best performance. Subsequently, Li *et al.* (2000) presented an experimental investigation on the singular perturbation-based tracking control of a two-link flexible manipulator. This approach has also proved to be successful in the modelling and controller design of flexible joint manipulators (Spong 1987, Khorasani 1992). From these investigations, it is clear that fairly accurate tracking with stabilization of elastic vibration due to either the link or joint is possible through the simple feedback design of reduced order two-time-scale models. Therefore, there is motivation to extend the technique to the case of manipulators with flexible links and joints in which rigid and flexible modes have different speed characteristics. However, there has been very little work reported on the control of flexible link and joint manipulators using the singular perturbation approach. Hence, in this paper, the singular perturbation technique is used for splitting the full order dynamic model of the flexible link and joint manipulator into two reduced order systems comprising one slow rigid subsystem and one fast flexible subsystem. The slow subsystem involves the joint variables as the slow state variables and the fast subsystem contains the generalized flexible coordinates and the joint flexibility as the fast state variables. Then, a composite controller is designed to control these two separate time-scale subsystems, such that when it is applied to the manipulator with coupled rigid and flexible dynamics, the desired trajectory will be tracked with simultaneous control of link and joint vibrations. In the first instance, a singular perturbation-based composite controller for this manipulator using reduced order models is designed, where the slow control design uses the computed torque technique and the fast control is based on a LQR approach. This control scheme, which we call singular perturbation computed torque (SPCT) control.

The use of the inverse dynamics technique for controlling the slow dynamics in the SPCT is based on the assumption of a perfect model. The gains of the controller are chosen to achieve a critically damped system response. However, because of unmodelled high frequency modes, the model uncertainty can also be reflected into the slow dynamics along with the inexactness due to the approximation of manifold expansion (Moallem *et al.* 1997). Hence, the ideal error response in the design of the controller for the slow subsystem may not be achieved in this situation and therefore good performance is not always guaranteed. Thus, there is a necessity to design robust control for the slow dynamics. In view of the above, a singular perturbation-based neurocontroller (SPNN) formulation has been made subsequently to cope with the model uncertainty. It has been reported that neural networks (NNs) offer exciting scope for designing improved control schemes because of their different salient features such as non-linear functional approximation, learning, adaptation, generalization and inherent parallelism (Lewis *et al.* 1995). Non-linear functions can be approximated by NNs to any desired degree of accuracy, enabling them to model non-linear systems for control design. During the past several years, there has been a lot of interest in applying neural networks to solve problems in identification and control of complex non-linear systems including robotic systems (Lewis *et al.* 1995, Ge *et al.* 1998). There are many situations where it is very difficult to get *a priori* knowledge of the dynamics of the system. These problems have been addressed successfully by

neural networks, where the structure of the controller does not depend on the system dynamics but rather on the filtered error. Therefore, in this paper, an NN-based control is used to replace the inverse dynamics control for the slow dynamics to tackle the model uncertainties. It is well known that the radial basis function neural networks offer some attractive features in contrast to multilayered perceptron neural networks such as the formers are bounded, strictly positive and absolutely integrable on $\Re^n$ (Ge *et al*. 2001a) and therefore used here for slow subsystem control design. The fast subsystem controller for the SPNN uses the state feed control based on LQR.

The paper is organized as follows. Section 2 presents the development of the non-linear dynamic model of the flexible link and flexible joint manipulator (FLFJM), which follows an Euler–Lagrange, assumed mode principle. In Section 3, the earlier control technique, i.e. the modified computed torque (MODCT) control for tracking a desired trajectory and compensating the link and joint flexibility simultaneously as proposed by Gogate and Lin (1993) for such a manipulator is reviewed. Section 4 discusses the formulation of the two-time-scale singular perturbation model of the FLFJM that has been obtained in Section 2. Section 5 presents the design of a composite control based on the resulting reduced order model of the FLFJM, where the slow control design uses the computed torque technique and the fast control is based on an LQR approach (SPCT). Section 6 deals with the development of an improved controller using neural network-based slow control and a state feedback LQ control (SPNN). Results and concluding remarks are given in Sections 7 and 8, respectively.

2. Dynamical modelling of the manipulator

Figure 1 shows the schematic diagram of a FLFJM considered here. It consists of one flexible link of uniform cross-sectional area and one flexible joint. The arm is powered by a motor and moves in a horizontal plane. The flexible joint, dynamically simplified as a linear torsional spring, works as a connector between the motor and the robot arm. Let, OX_0Y_0 be the inertial coordinate frame and OXY be the moving frame. The clamped end of the flexible arm of length l, uniform flexural rigidity EI, mass m and the mass moment of inertia I_b, is attached to the hub of inertia I_h and connected to the rotor with inertia I_r, and gear ratio G, where an input torque u is applied to move the link and the end-effector carries a payload mass, m_p.

The manipulator is assumed to operate on the horizontal plane so that the effect of gravity is ignored. The effects of rotary inertia and shear deformation are ignored by assuming that the cross-sectional area of the link is small in comparison with its length l. The Euler–Bernoulli beam theory and the assumed modes method can be used to express the deflection $v(x, t)$ of a point located at a distance x along the arm as (Meirovitch 1986):

$$v(x,t) = \sum_{i=1}^{n} \phi_i(x) q_i(t) \tag{1}$$

where $\phi_i(x)$ is the mode shape function, $q_i(t)$ is the time varying modal function and n is the number of finite modes.

To derive the dynamic equations of the motion of the FLFJM, we need to compute the total energy associated with the system as follows. The total kinetic energy of the flexible manipulator system is due to the motion of the link, hub and rotor and due to the kinetic energy associated with the payload, i.e.:

$$T = T_h + T_l + T_r + T_p \tag{2}$$

where T_h, T_l, T_r and T_p are the kinetic energy of the hub, link, rotor and the payload, respectively. The kinetic energy due to the motion of the hub can be written as:

$$T_h = \frac{1}{2} I_h \dot{\theta}^2. \tag{3}$$

The kinetic energy of the rotor is given by:

$$T_r = \frac{1}{2} J \dot{\alpha}^2, \tag{4}$$

where $J = G^2 I_r$. The kinetic energy due to the motion of the link can be expressed as:

$$T_l = \frac{1}{2} \rho \int_0^l \dot{\boldsymbol{r}}^T \dot{\boldsymbol{r}} \mathrm{d}x. \tag{5}$$

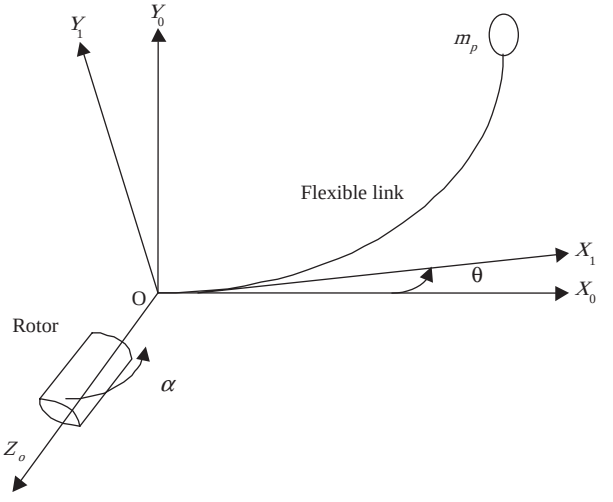

Figure 1. Schematic diagram of the flexible-link and joint manipulator.

In figure 1, $\boldsymbol{r}$ denotes the position vector of a point x on the arm with respect to the Cartesian coordinate system (OX_0Y_0) and $\boldsymbol{r}^*$ is the position vector with respect to (OXY). Then, $\boldsymbol{r}(\theta, x, t)$ can be written using simple geometry as:

$$\boldsymbol{r}(\theta, x, t) = \begin{bmatrix} \cos\theta & -\sin\theta \\ \sin\theta & \cos\theta \end{bmatrix} \begin{bmatrix} x \\ v(x,t) \end{bmatrix}. \tag{6}$$

From equation (8) we get:

$$\dot{\boldsymbol{r}}(\theta, x, t) = \begin{bmatrix} \cos\theta & -\sin\theta \\ \sin\theta & \cos\theta \end{bmatrix} \begin{bmatrix} -\dot{v}(x,t) \\ x\dot{\theta} + \dot{v}(x,t) \end{bmatrix}. \tag{7}$$

Substituting $\dot{\boldsymbol{r}}(\theta, x, t)$ from equation (7) into equation (5) we get:

$$T_l = \frac{1}{2}\rho \int_o^l [v^2(x,t)\dot{\theta}^2 + x^2\dot{\theta}^2 + \dot{v}^2(x,t) + 2x\dot{\theta}\dot{v}(x,t)]\mathrm{d}x \tag{8}$$

Similarly, the kinetic energy associated with the payload can be written as:

$$T_p = \frac{1}{2} m_p \left\{ v^2(x,t)|_{x=l}\dot{\theta}^2 + l^2\dot{\theta}^2 + \dot{v}^2(x,t)|_{x=l} + 2l\dot{\theta}\dot{v}(x,t)|_{x=l} \right\}. \tag{9}$$

The total potential energy V of the system can be written as:

$$V = V_{el} + V_j, \tag{10}$$

where V_{el} is the potential energy resulting from the elastic deformation of the link and V_j is due to the joint deflection. The potential energy due to the elastic deflection of the link is given by:

$$V_{el} = \frac{1}{2}\int_0^l EI\left(\frac{\partial^2 v(x,t)}{\partial x^2}\right)^2 \mathrm{d}x. \tag{11}$$

Let K_s be the spring constant of the joint. Then potential energy of the joint can be written as:

$$V_j = \frac{1}{2} K_s(\alpha - \theta)^2. \tag{12}$$

Now, the above expressions for the kinetic and potential energy due to the link deflection can be discretized using the assumed mode method by substituting for $v(x,t)$ from equation (1).

Using the boundary and orthogonality conditions for a clamped-mass configuration the mode shapes can be obtained as below (Chapnik *et al.* 1991):

$$\begin{aligned} \phi_i(x) = A_i \Bigg\{ & \cosh\frac{\lambda_i x}{l} - \cos\frac{\lambda_i x}{l} \\ & - \gamma\left(\sinh\frac{\lambda_i x}{l} - \sin\frac{\lambda_i x}{l}\right)\Bigg\} = A_i\psi_i(x), \end{aligned} \tag{13}$$

where $\gamma_i = (\cosh\lambda_i + \cos\lambda_i)/(\sinh\lambda_i + \sin\lambda_i)$, λ_i is the Eigen value of the link and A_i is the normalization constant for incorporating the effect of the payload in the mode shape function for the clamped-free case, which is taken as below (Chapnik *et al.* 1991):

$$A_i = \left[\int_0^l \psi_i^2(x)\mathrm{d}x + \frac{m_p}{m}\psi_i^2(l)\right]^{-1/2}. \tag{14}$$

The frequency of natural vibration $\omega_i = \lambda_i^2\sqrt{EI/\rho}$ is obtained through determination of λ_i from:

$$1 + \cosh\lambda_i\cos\lambda_i + \frac{m_p}{m}(\sinh\lambda_i - \cosh\lambda_i\sin\lambda_i) = 0. \tag{15}$$

Having determined the assumed spatial mode shapes $\phi_i(x)$, the associated time varying modal variables $q_i(t)$ in equation (1) are being considered as one of the components in the generalized coordinates of the flexible link and joint manipulator system (Gogate and Lin 1993, Geniele *et al.* 1997) as described below.

The dynamic equations of the system can be derived using the Lagrangian equation:

$$\frac{\mathrm{d}}{\mathrm{d}t}\left[\frac{\partial L}{\partial Q_i}\right] - \frac{\partial L}{\partial Q_i} = F_i, \quad L = T - V, \tag{16}$$

where the Lagrangian, L, can be determined by substituting equation for the total kinetic energy and the total potential energy from equations (2) and (10), respectively. The generalized coordinate vector, $Q = \{Q_i\}$ consists of the rotor angle, link angle and the modal variables, i.e.:

$$Q = \begin{bmatrix} \alpha & \theta & q_1 & q_2 & \cdots & q_n \end{bmatrix}^{\mathrm{T}},$$

and the corresponding generalized force vector, $F = \{F_i\}$, is given by:

$$F = \begin{bmatrix} u & 0 & 0 & 0 & \cdots & 0 \end{bmatrix}^{\mathrm{T}},$$

where u is the torque applied by the rotor. Equation (16) can be expanded into the following set of equations in terms of the separate components of Q_i and F_i:

$$\frac{\mathrm{d}}{\mathrm{d}t}\left[\frac{\partial L}{\partial \dot{\alpha}}\right] - \frac{\partial L}{\partial \alpha} = u, \quad \frac{\mathrm{d}}{\mathrm{d}t}\left[\frac{\partial L}{\partial \dot{\theta}}\right] - \frac{\partial L}{\partial \theta} = 0,$$
$$\text{and} \quad \frac{\mathrm{d}}{\mathrm{d}t}\left[\frac{\partial L}{\partial \dot{q}_i}\right] - \frac{\partial L}{\partial q_i} = 0.$$

After some algebraic manipulations, the dynamic equations of the flexible link and joint manipulator can be concisely written as:

$$J\ddot{\alpha} - K_s(\theta - \alpha) = u \tag{17}$$

$$D(\theta,q)\begin{bmatrix}\ddot{\theta}\\ \ddot{q}\end{bmatrix} + \begin{bmatrix}g_1(\theta,\dot{\theta},q,\dot{q})\\ g_2(\theta,\dot{\theta},q,\dot{q})\end{bmatrix} + \begin{bmatrix}-K_s(\alpha-\theta)\\ K_w q\end{bmatrix} = \begin{bmatrix}0\\0\end{bmatrix}, \tag{18}$$

where the inertia matrix D is:

$$D = \begin{bmatrix} I_h + I_b + \rho\int_0^l \phi_i^2 \mathrm{d}x q_i^2 + m_p(l^2 + \phi_i(l)\phi_j(l)q_i & \rho\int_0^l x\phi_1 \mathrm{d}x + m_p l\phi_1(l) & \cdot & \rho\int_0^l x\phi_n \mathrm{d}x + m_p l\phi_n(l) \\ \rho\int_0^l x\phi_1 \mathrm{d}x + m_p l\phi_1(l) & \rho + m_p\phi_1^2(l) & \cdot & m_p\phi_1(l)\phi_n(l) \\ \cdot & \cdot & \cdot & \cdot \\ \rho\int_0^l x\phi_n \mathrm{d}x + m_p l\phi_n(l) & m_p\phi_n(l)\phi_1(l) & \cdot & \rho + m_p\phi_n^2(l) \end{bmatrix}$$

and the vectors containing the coupling between the rigid and elastic variables are:

$$g_1 = 2\rho\int_0^l \phi_i^2 \mathrm{d}x q_i\dot{q}_i\dot{\theta} + m_p\phi_i(l)\phi_j(l)(\dot{q}_i q_j + q_i\dot{q}_j)\dot{\theta}$$

$$g_2 = \begin{bmatrix} -\dot{\theta}^2\rho\int_0^l \phi_1^2 \mathrm{d}x - m_p\dot{\theta}^2(\phi_1^2(l)q_1 + \phi_1(l)\phi_2(l)q_2 + \cdots + \phi_1(l)\phi_n(l)q_n) \\ -\dot{\theta}^2\rho\int_0^l \phi_2^2 \mathrm{d}x - m_p\dot{\theta}^2(\phi_1(l)\varphi_2(l)q_1 + \phi_2^2(l)q_2 + \cdots + \phi_2(l)\phi_n(l)q_n) \\ \cdot \\ -\dot{\theta}^2\rho\int_0^l \phi_n^2 \mathrm{d}x - m_p\dot{\theta}^2(\phi_n(l)\phi_1(l)q_1 + \phi_n(l)\phi_2(l)q_2 + \cdots + \phi_n^2(l)q_n) \end{bmatrix}.$$

The stiffness matrix K_w is written as $K_w = \mathrm{diag}(k_1, k_2, \ldots, k_n)$, where $k_i = \omega_i^2 m$.

3. Modified computed control scheme

Figure 2 gives the modified computed control (MODCT) scheme that uses inverse dynamics control along with a correction for joint flexibility as proposed by Gogate and Lin (1993). It is explained in brief here.

Equations (17) and (18) can be rewritten as:

$$J\ddot{\alpha} + K_s\delta = u \tag{19}$$

$$\begin{bmatrix}D_{11} & D_{12}\\ D_{21} & D_{22}\end{bmatrix}\begin{bmatrix}\ddot{\theta}\\ \ddot{q}\end{bmatrix} + \begin{bmatrix}g_1\\ g_2\end{bmatrix} + \begin{bmatrix}-K_s\delta\\ K_w q\end{bmatrix} = \begin{bmatrix}0\\0\end{bmatrix}, \tag{20}$$

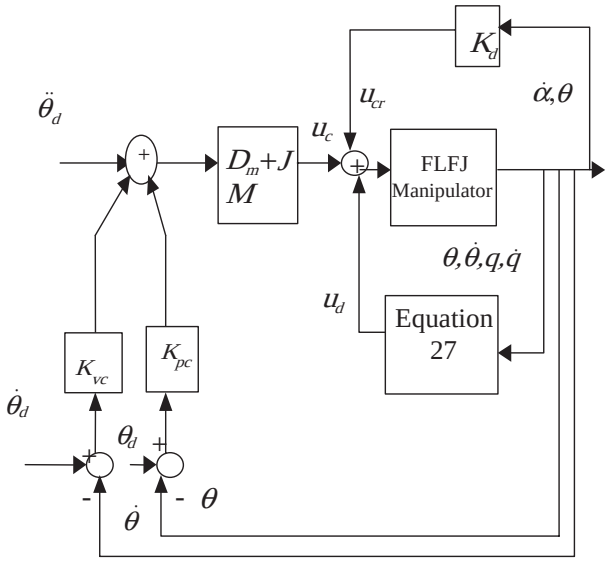

Figure 2. Block diagram for the modified computed torque controller.

where $\delta = (\alpha - \theta)$ and $D^{-1}(\theta,q) = H(\theta,q) = \begin{bmatrix}H_{11}(\theta,q) & H_{12}(\theta,q)\\ H_{21}(\theta,q) & H_{22}(\theta,q)\end{bmatrix}$. From equation (20):

$$\ddot{q} = H_{22}(-K_w q - g_2 - D_{21}\ddot{\theta}) \tag{21}$$

$$D_{11}\ddot{\theta} + D_{12}\ddot{q} - K_s\delta + g_1 = 0 \tag{22}$$

Now, $\ddot{q}$ from equation (21) is substituted in equation (22) to give:

$$D_{11}\ddot{\theta} + D_{12}H_{22}\{-K_w q - g_2 - D_{21}\ddot{\theta}\} - K_s\delta + g_1 = 0. \tag{23}$$

After simplifying, equation (23) can be expressed as:

$$D_m\ddot{\theta} + u_d - K_s\delta = 0, \tag{24}$$

where

$$D_m = \{D_{11} - D_{12}H_{22}D_{21}\} \tag{25}$$

$$u_d = -D_{12}H_{22}K_w q - D_{12}H_{22}g_2 + g_1 \tag{26}$$

A joint damping term, $K_d(\dot{\theta} - \dot{\alpha})$, could be introduced into the closed-loop system to damp out the joint oscillations (Spong 1987), which gives rise to a correction torque u_{cr} for controlling the joint flexibility as

$$u_{cr} = K_d(\dot{\theta} - \dot{\alpha}), \tag{27}$$

where K_d is a constant gain.

Assuming that a torque as given in equation (27) is applied to compensate for joint flexure disturbance, the dynamic equation of the manipulator with flexible link and flexible joint reduces to:

$$(D_m + J)\ddot{\theta} + u_d = 0 \tag{28}$$

To control the vibration of the links and track the desired trajectory, a computed torque control is to be developed as follows. The position and velocity tracking errors can be defined as:

$$e(t) = \theta_d(t) - \theta(t) \quad \text{and} \quad \dot{e}(t) = \dot{\theta}_d(t) - \dot{\theta}(t). \tag{29}$$

$\theta_d(t)$ and $\dot{\theta}_d(t)$ are the position and velocity of the desired trajectory. Therefore, the computed torque $u_c(t)$ can be obtained as:

$$u_c(t) = (D_m + J)\big(\ddot{\theta}_d(t) + K_{pc}e(t) + K_{vc}\dot{e}(t)\big) + u_d(t), \tag{30}$$

where K_{pc} and K_{vc} are the position and velocity gains, respectively, of the computed torque controller. Therefore, combining the control signals given in equations (29) and (30), the net torque can be obtained as:

$$u(t) = u_c(t) + u_{cr}(t). \tag{31}$$

4. Singular perturbation modelling of the manipulator

In this section, the dynamic model of a manipulator with flexible link and joint is converted into a two-time-scale singular perturbation model. Note that a singular perturbation model for a system is not unique. For example, in the case of *rigid-* and *flexible-joint* manipulators, two types of singular perturbation models have been reported. The first considers the elastic forces, i.e. $k_s(\alpha - \theta)$ and $k_s(\dot{\alpha} - \dot{\theta})$ as the fast variables, and the link angular positions as the slow variables (Spong 1987), while the second singular perturbation model assumes the motor tracking errors as the fast variables instead of the joint elastic forces (Ge and Postlethwaite 1995). However, in both the cases the inverse of the spring constant is chosen as the perturbation parameter. In the case of flexible- and rigid-joint manipulators, Siciliano and Book (1988) and Siciliano *et al.* (1992) have chosen a common scale factor among the stiffness constants of the different modes of the links. They then used the inverse of this scale factor as the perturbation parameter to formulate a two-time-scale singular perturbation model from the Euler–Lagrange flexible manipulator dynamics. Aoustin and Chevallereau (1993) developed a singular perturbation model by considering the tip displacement and the rotations as the fast variables, and extracted the minimum of the inverse of the stiffness constants as the perturbation parameter. However, Vandergrift *et al.* (1994) formulated a singular perturbation model after performing an input and output feedback linearization of the flexible link manipulator dynamics, and accordingly considered the transformed stiffness matrix for selecting the perturbation parameter. For the flexible-link and -joint manipulator, a perturbation parameter is selected as follows. Let k_c be a common scale factor amongst all the stiffness constants of the link and joint (torsional spring constants, k_s of the joints, and the flexural spring constants, K_w of the link). The inverse of this scale factor is chosen as a perturbation parameter.

The dynamic model of the FLFJM obtained in Section 2 is transformed into a two-time-scale singular perturbation model as described below. $\ddot{\theta}$ and $\ddot{q}$ can be determined from equations (19) and (20) as follows:

$$\ddot{\theta} = -H_{11}(\theta, q)g_1(\theta, \dot{\theta}, q, \dot{q}) - H_{12}(\theta, q)g_2(\theta, \dot{\theta}, q, \dot{q}) + H_{11}(\theta, q)K_s\delta - H_{12}(\theta, q)K_w q \tag{32}$$

$$\ddot{q} = -H_{21}(\theta, q)g_1(\theta, \dot{\theta}, q, \dot{q}) - H_{22}(\theta, q)g_2(\theta, \dot{\theta}, q, \dot{q}) - H_{22}(\theta, q)K_w q + H_{21}(\theta, q)K_s\delta \tag{33}$$

From equation (19):

$$\ddot{\delta} = \ddot{\alpha} - \ddot{\theta} = -J^{-1}K_s\delta + J^{-1}u - \ddot{\theta}. \tag{34}$$

We define a common scale factor k_c, which is the minimum of all the stiffness constants, i.e. $k_c = \min(k_1, k_2, \ldots, k_n, K_s)$. With this common scale factor, the torsional spring constant K_s and the flexural spring constant K_w can be scaled by k_c, such that $\tilde{K}_s = K_s/k_c$ and $\tilde{K}_w = K_w/k_c$.

Now defining $\tau_q = k_c q$, $\tau_\delta = k_c \delta$, $\mu = 1/k_c$ and substituting, $q = \mu\tau_q$ and $\delta = \mu\tau_\delta$ into equations (32–34), we get:

$$\begin{aligned}\ddot{\theta} = &-H_{11}(\theta, \mu\tau_q)g_1(\theta, \dot{\theta}, \mu\tau_q, \mu\dot{\tau}_q)\\ &- H_{12}(\theta, \mu\tau_q)g_2(\theta, \dot{\theta}, \mu\tau_q, \mu\dot{\tau}_q)\\ &- H_{12}(\theta, \mu\tau_q)\tilde{K}_w\tau_q + H_{11}(\theta, \mu\tau_q)\tilde{K}_s\tau_\delta \end{aligned} \tag{35}$$

$$\begin{aligned}\mu\ddot{\tau}_q = &-H_{21}(\theta, \mu\tau_q)g_1(\theta, \dot{\theta}, \mu\tau_q, \mu\dot{\tau}_q)\\ &- H_{22}(\theta, \mu\tau_q)g_2(\theta, \dot{\theta}, \mu\tau_q, \mu\dot{\tau}_q)\\ &- H_{22}(\theta, \mu\tau_q)\tilde{K}_w\tau_q + H_{21}(\theta, \mu\tau_q)\tilde{K}_s\tau_\delta \end{aligned} \tag{36}$$

$$\mu\tau_\delta = -J^{-1}\tilde{K}_s\tau_\delta + J^{-1}u - \ddot{\theta}. \tag{37}$$

To obtain, the slow and fast subsystems for the singular perturbation model of the flexible link and joint manipulator, μ is set to zero (Siciliano and Book 1988) in equations (35–37). Solving for $\bar{\tau}_q$and $\bar{\tau}_\delta$ then yields (using the 'overbar' to indicate the value of the variable at $\mu = 0$):

$$\bar{\tau}_\delta = \tilde{K}_s^{-1}(\bar{u} - J\ddot{\bar{\theta}}) \tag{38}$$

$$\bar{\tau}_q = \tilde{K}_w^{-1}H_{22}^{-1}H_{21}(\bar{u} - J\ddot{\bar{\theta}}). \tag{39}$$

Substitution of equations (38) and (39) into the equation (35) gives:

$$\ddot{\bar{\theta}} = [H_{11}(\overline{\theta}, 0) - H_{12}(\bar{\theta}, 0)H_{22}(\bar{\theta}, 0)H_{21}(\bar{\theta}, 0)] \times \{\bar{u} - J\ddot{\theta}\}. \tag{40}$$

Note that $[H_{11}(\bar{\theta}, 0) - H_{12}(\bar{\theta}, 0)H_{22}(\bar{\theta}, 0)H_{21}\bar{\theta}, 0)] = D_{11}^{-1}(\bar{\theta})$. Therefore, equation (40) can be rewritten as:

$$\ddot{\bar{\theta}} = (D_{11} + J)^{-1} \times \bar{u}, \tag{41}$$

where D_{11} is the first *block* of the mass matrix D of the FLFJM. Note that in the case of a single-link flexible manipulator D_{11} is a scalar. Equation (41), which represents the dynamics of the slow subsystem of the FLFJM, is similar to the equation for the rigid link and rigid joint manipulator.

Our purpose is now to convert the singular perturbation model of the FLFJM given through equations (35–37) into state-space form as follows. We choose the following state variables to obtain the boundary layer correction (Siciliano *et al.* 1992):

$$x_1 = \theta, \quad x_2 = \dot{\theta}, \quad z_1 = \tau_q, \quad z_2 = \varepsilon\dot{\tau}_q,$$
$$y_1 = \tau_\delta, \quad \text{and} \quad y_2 = \varepsilon\dot{\tau}_\delta,$$

where $\varepsilon = \sqrt{\mu}$.

Then, using the above state variables in the equations (35–37), the following state-space representation of the singular perturbation model is obtained:

$$\left.\begin{aligned}\dot{x}_1 &= x_2\\ \dot{x}_2 &= -H_{11}(x_1, \varepsilon^2 z_1)g_1(x_1, x_2, \varepsilon^2 z_1, \varepsilon z_2)\\ &\quad - H_{12}(x_1, \varepsilon^2 z_1)g_2(x_1, x_2, \varepsilon^2 z_1, \varepsilon z_2)\\ &\quad - H_{12}(x_1, \varepsilon^2 z_1)z_1 + H_{11}(x_1, \varepsilon^2 z_1)y_1\end{aligned}\right\} \tag{42}$$

$$\left.\begin{aligned}\varepsilon\dot{z}_1 &= z_2\\ \varepsilon\dot{z}_2 &= -H_{21}(x_1, \varepsilon^2 z_1 x_1, \varepsilon^2 z_1)g_1(x_1, x_2, \varepsilon^2 z_1, \varepsilon z_2)\\ &\quad - H_{22}(x_1, \varepsilon^2 z_1)g_2(x_1, x_2, \varepsilon^2 z_1, \varepsilon z_2)\\ &\quad - H_{22}(x_1, \varepsilon^2 z_1)z_1 + H_{21}(x_1, \varepsilon^2 z_1)y_1\end{aligned}\right\} \tag{43}$$

$$\left.\begin{aligned}\varepsilon\dot{y}_1 &= y_2\\ \varepsilon\dot{y}_2 &= -J^{-1}\tilde{K}_s y_1 + J^{-1}(u - J\dot{x}_2)\end{aligned}\right\}. \tag{44}$$

On setting $\varepsilon = 0$ (Siciliano and Book 1988) in equation (42), the slow subsystem in the state-space form can be written as:

$$\left.\begin{aligned}\dot{\bar{x}}_1 &= \bar{x}_2\\ \dot{\bar{x}}_2 &= (D_{11} + J)^{-1}\bar{u}\end{aligned}\right\} \tag{45}$$

Now to obtain the fast subsystem, a fast time scale defined by $t_f = t/\varepsilon$ is introduced. Note that, at the boundary layer $\varepsilon = 0$, $\mathrm{d}x_1/\mathrm{d}t_f$, $\mathrm{d}x_2/\mathrm{d}t_f$; $g_1(x_1, x_2, 0, 0)$ and $g_2(x_1, x_2, 0, 0)$ are zero. Hence in the fast time scale, defining new fast variables as:

$$n_{q^1} = z_1 - \bar{\tau}_q; \quad n_{q^2} = z_2; \quad n_{a^1} = y_1 - \bar{\tau}_\delta; \quad n_{a^2} = y_2 \tag{46}$$

and with substitution of these fast variables corresponding to the state variables y_1, y_2, z_1 and z_2 in equations (42–44), the fast subsystem can be determined as follows:

$$\left.\begin{aligned}\frac{\mathrm{d}\eta_{q^1}}{\mathrm{d}t_f} &= \eta_{q^2}\\ \frac{\mathrm{d}\eta_{q^2}}{\mathrm{d}t_f} &= -H_{22}(\bar{x}_1, 0)\tilde{K}_w\eta_{q^1} + H_{21}(\bar{x}_1, 0)\eta_{a^1}\\ \frac{\mathrm{d}\eta_{a^1}}{\mathrm{d}t_f} &= \eta_{a^2}\\ \frac{\mathrm{d}\eta_{a^2}}{\mathrm{d}t_f} &= -J^{-1}\tilde{K}_s\eta_{a^1} + J^{-1}K_s u_f\end{aligned}\right\}, \tag{47}$$

which can be rewritten as:

$$\dot{x}_f = A_f x_f + B_f u_f, \tag{48}$$

where

$$A_f = \begin{bmatrix} 0 & 0 & 0 & I\\ H_{22}\tilde{K}_w & H_{21}\tilde{K}_s & 0 & 0\\ 0 & 0 & J^{-1}\tilde{K}_s & 0\end{bmatrix} \quad \text{and} \quad B_f = \begin{bmatrix} 0\\ J^{-1}\end{bmatrix},$$

the 0 and I matrices are of appropriate dimensions.

5. Design of the singular perturbation control using the computed torque technique

Figure 3 gives the structure for the singular perturbation-based computed torque and linear-quadratic controller (SPCT). On the basis of the two-time scale, slow and fast subsystems of the flexible link and joint manipulator as derived above (equations 45 and 47, respectively), a composite control can be obtained as (Kokotovic 1984):

$$u = u_s + u_f, \tag{49}$$

where u_s is the slow control and u_f is the fast control, respectively, and the fast control is designed such that at $\varepsilon = 0$ that u_f becomes zero.

The slow control for the slow subsystem (45) can be designed according to the well-known computed torque control technique used for rigid manipulators:

$$u_s = (D_{11} + J)\{\ddot{\theta}_d(t) + K_p(\theta_d - \theta) + K_v(\dot{\theta}_d - \theta)\}, \tag{50}$$

where K_P and K_v are the controller gains and θ_d is the desired trajectory.

As the pair (A_f, B_f) of the fast subsystem given in equation (48) is found to be completely state controllable, therefore, a fast state feedback control can be devised to force the states x_f to zero:

$$u_f = -K_f x_f, \tag{51}$$

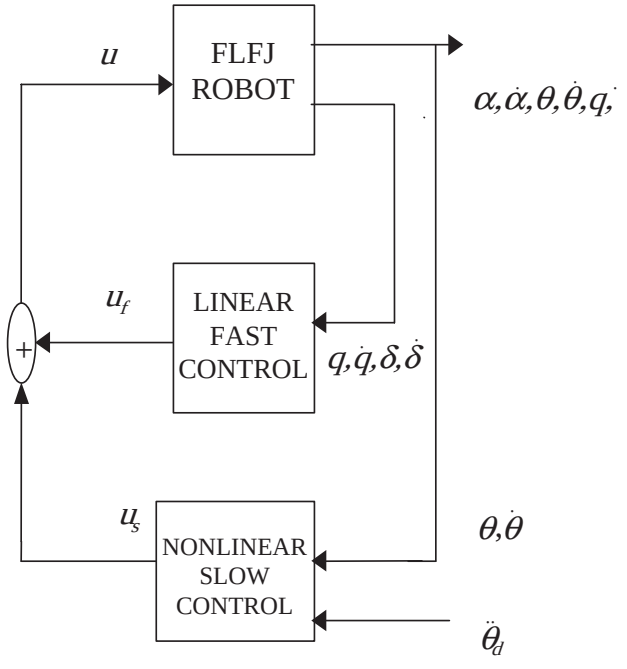

Figure 3. Structure of the singular perturbation controller with computed torque for slow dynamics.

where the feedback gains K_f are obtained through optimizing the cost function given below through an LQR approach:

$$J_f = \frac{1}{2}\int_0^\infty \left[x_f^{\mathrm{T}}(t)Qx_f + u_f^{\mathrm{T}}(t)Ru_f(t)\right]\mathrm{d}t. \tag{52}$$

6. Design of the RBFNN-based composite control scheme

Figure 4 shows the structure of the singular perturbation neurocontroller (SPNN). In this case, the composite control signal (u) is the combination of slow and fast subsystem control actions denoted, respectively, by $\bar{u}$ and u_f, where $\bar{u}$ is obtained as:

$$\bar{u} = u_{NN} + K_n e_f(t) \tag{53}$$

and u_{NN} is the control signal generated using the radial basis function neural networks, K_n is the gain of the controller and $e_f(t)$ is the filtered tracking error. Stabilization of the fast subsystem is achieved through a linear state-feedback control principle as described in Section 5.

6.1. *Radial basis neural network controller for the slow subsystem*

The approximation capabilities of neural networks have been used to learn non-linear characteristics of many systems (Sanner and Slotine 1992). In particular, the Gaussian radial basis function neural network can approximate any function (Haykins 1998).

Referring to figure 5, for a given smooth function, $f(x) : \Re^{n_i} \to \Re^{n_o}$, there exist optimal parameters $w_{kj} \in \Re$ such that:

$$\hat{f}_k(x) = \sum_j^{n_h} w_{kj}a_j(x) = w_k^{\mathrm{T}}a(x) \quad k = 1, 2, \ldots, n_o \tag{54}$$

$$\hat{f}(x) = \left[\hat{f}_1(x) \quad \cdot \quad \hat{f}_k(x) \quad \cdot \quad \hat{f}_{n_o}(x)\right]^{\mathrm{T}}, \tag{55}$$

$$f(x) = \hat{f}(x) + \Xi(x), \tag{56}$$

where $\Xi(x)$ is the minimum approximation error and $a_j(x), (j = 1, 2, \ldots, n_h)$ are the Gaussian functions defined as:

$$a_j(x) = \exp\left(-\frac{(x - \overline{\lambda}_j)^{\mathrm{T}}(x - \overline{\lambda}_j)}{\sigma_j^2}\right), \tag{57}$$

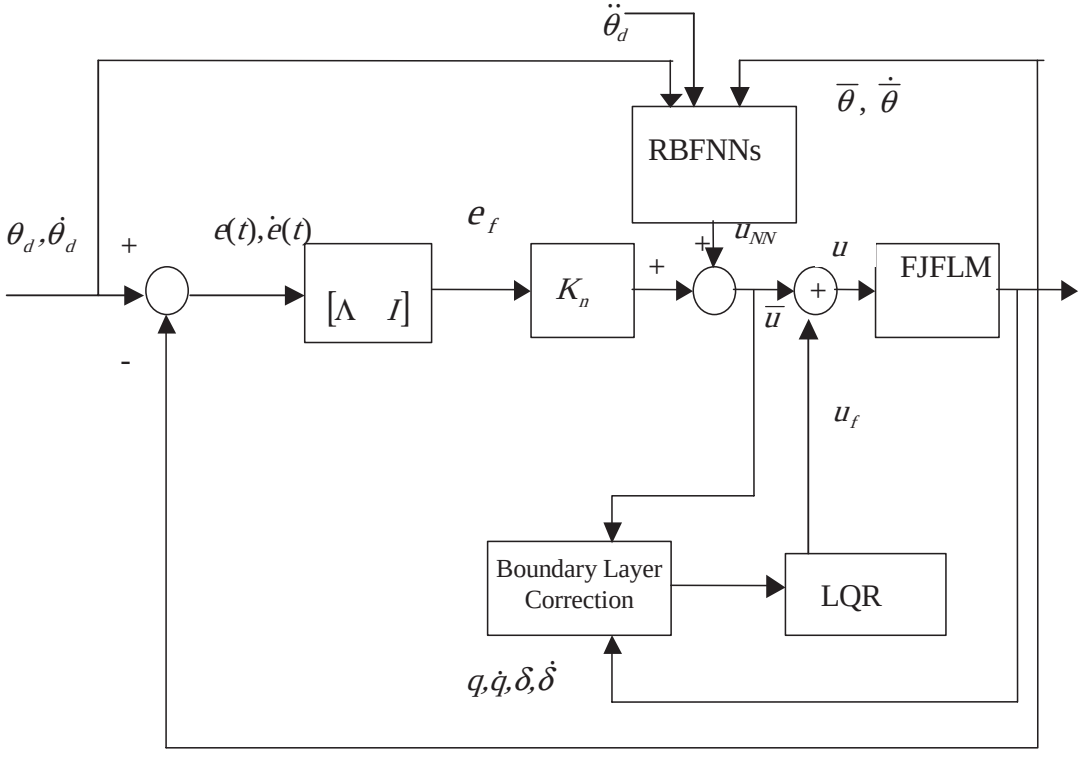

Figure 4. Structure of the singular perturbation controller with neural networks applied to slow dynamics.

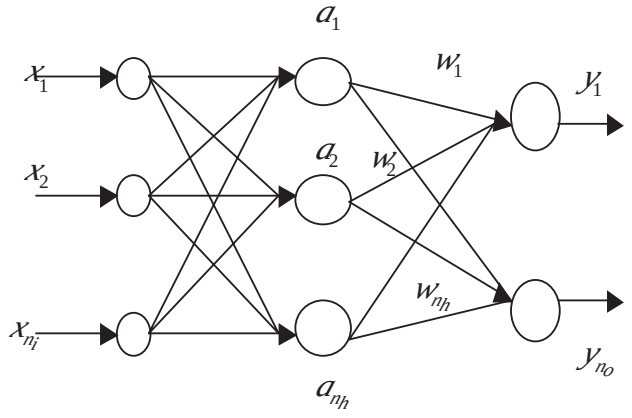

Figure 5. Radial basis function neural network.

where $\bar{\lambda}_j \in \Re^n$ is the centre vector of the hidden unit with the same dimension as the input vector x, and σ_j^2 is the variance of each defined Gaussian basis function.

Let $\theta_d(t) \in \Re^n$ be the given trajectory, which is assumed to be at least twice differentiable. Define the trajectory tracking error, $e(t)$ and the filtered tracking error $e_f(t)$ as:

$$e(t) = \theta_d(t) - \bar{\theta}(t), \tag{58}$$

$$e_f(t) = \dot{\theta}_s(t) - \dot{\bar{\theta}}(t), \tag{59}$$

where $\dot{\theta}_s(t) = \dot{\theta}_d(t) + \Lambda e(t)$ with Λ being a symmetric positive definite constant matrix. Therefore, from equations (58) and (59) we obtain:

$$\dot{\bar{\theta}}(t) = \dot{\theta}_s(t) - e_f(t); \ddot{\bar{\theta}}(t) = \ddot{\theta}_s(t) - \dot{e}_f(t) \tag{60}$$

and also the filtered tracking error as:

$$e_f(t) = \dot{e}(t) + \Lambda e(t). \tag{61}$$

The slow subsystem of the two-time-scale perturbed model for the flexible link and flexible joint manipulator given in equation (41) can be rewritten as:

$$M(\bar{\theta})\ddot{\bar{\theta}} = \bar{u}, \tag{62}$$

where $D_{11} + J = M$. Note that there is some uncertainty in M owing to the inexact time-scale separation (Moallem *et al.* 1997). The elements of $M(\bar{\theta})$, i.e. $m_{ij}(\bar{\theta})$, are functions of $\bar{\theta}$ only and are infinitely differentiable. Therefore, neural networks with inputs $\bar{\theta}$ only are sufficient to model them. By using the RBFNNs, $m_{ij}(\bar{\theta})$ can be approximated as:

$$m_{ij}(\bar{\theta}) = W_{ij}^{\mathrm{T}} \xi_{ij}(\bar{\theta}) + \varepsilon_{M_{ij}}, \tag{63}$$

where W_{ij}, $\xi_{ij}(\bar{\theta})$ and $\varepsilon_{M_{ij}}$, respectively, denote weight vector, vector of activation functions and NN approximation errors. The elements of $\xi_{ij}(\bar{\theta})$ are the Gaussian RBFs and can be written as:

$$\xi_{ij}(\bar{\theta}) = \exp\left(-\frac{(\bar{\theta}-\overline{\lambda}_{ij})^{\mathrm{T}}(\bar{\theta}-\overline{\lambda}_{ij})}{\sigma_{ij}^2}\right). \tag{64}$$

Using GL matrix, $\{\cdot\}$ and GL operator, $\bullet$ (Ge *et al.* 1998), the function emulator (63) can be represented as:

$$M(\bar{\theta}) = [\{W\}^{\mathrm{T}} \bullet \{\Xi\}] + E_M, \tag{65}$$

where $\{W\}$ and $\{\Xi\}$ are the desired parameter and basis function pair of the NN emulation of $M(\bar{\theta})$ and E_M is the collective NN reconstruction error vector. Let $\hat{M}(\bar{\theta})$ be the NN estimate of $M(\bar{\theta})$, which can be written as:

$$\hat{M}(\bar{\theta}) = [\{\hat{W}\}^{\mathrm{T}} \bullet \{\Xi\}], \tag{66}$$

where $\{\hat{W}\}$ is the NN weight vector.

Substituting $\ddot{\bar{\theta}}(t)$ from equation (60) and by using equation (65), the left-hand side of equation (62) can be expressed as:

$$M(\bar{\theta})\ddot{\bar{\theta}} = [\{W\}^{\mathrm{T}} \bullet \{\Xi\}]\ddot{\theta}_s + E_M\dot{\theta}_s - M(\bar{\theta})\dot{e}_f. \tag{67}$$

Consider the neural network-based controller for the slow subsystem to be of the form:

$$\bar{u} = u_{NN} + K_n e_f. \tag{68}$$

The first term in equation (68) is given by:

$$u_{NN} = \hat{M}(\theta)\ddot{\theta}_s. \tag{69}$$

After substitution of equation (66) in equation (69), $\bar{u}$ can be written as:

$$\bar{u} = \{\hat{W}\}^{\mathrm{T}} \bullet \{\Xi(\bar{\theta})\}\ddot{\theta}_s + K_n e_f. \tag{70}$$

Now by using equations (69) and (70) the closed-loop error equation can be derived as:

$$M(\bar{\theta})\dot{e}_f + K_n e_f = \{\tilde{W}\}^{\mathrm{T}} \bullet \{\Xi(\bar{\theta})\}\ddot{\theta}_s + E_M\dot{\theta}_s, \tag{71}$$

where $\tilde{W} = W - \hat{W}$. By using the following parameter adaptation law, the closed-loop system becomes asymptotically stable (Ge *et al.* 2001a):

$$\dot{\hat{W}}_i = \Gamma_{mi} \bullet \left\{\xi_{ij}(\bar{\theta})\right\}\ddot{\theta}_s e_{fi}, \tag{72}$$

where Γ_{mi} and W_i are symmetric positive definite matrices of appropriate dimensions.

7. Results and discussion

The proposed controllers were applied to a manipulator with one flexible link and one flexible joint. The nonlinear differential equation model given in equations (17) and (18) was simulated using a fourth-order Runge–Kutta integration method at a sampling rate of 1 ms. As the contributions from modes higher than two are considered to be very small and negligible (Cetinkunt and Yu 1991), only two modes of the elastic link vibrations are considered. The mechanical properties of the FLFJM are given in table 1.

The manipulator was commanded to track the desired trajectory which is smooth and continuous in position, velocity and acceleration as given below:

$$\theta_d(t) = \theta_i(t) + d_m\left(6\frac{t^5}{t_d^5} - 15\frac{t^4}{t_d^4} + 10\frac{t^3}{t_d^3}\right), \tag{73}$$

where $\theta_d(t)$ is the desired value, $\theta_i(t)$ is the initial value, t_d is the desired duration of motion and d_m is a constant, which is taken as $\pi/2$ radian. A joint motion is commanded from $\theta_i = 0$ radian to $\theta_d(t_d) = \pi/2$ radian, where $t_d = 4$ s.

The gains for the modified computed torque (MODCT) controller as described in Section 3 are set as follows: $K_{pc} = 2.0$, $K_{vc} = 1.1$ and $K_d = 2.0$. The gains K_P and K_v for the slow subsystem control of the singular perturbation controller (SPCT) are selected as 1.0 and 1.5 so as to maintain the time-scale separation between the slow and fast subsystem. Selecting $Q_f = (1000, 100, 100, 100, 100, 100)$ and $R_f = 500$, the gains K_f are obtained as follows for the fast controller. $K_f = \{0.6992, 0.4823, 13.4894, -0.0852, 0.1508, 7.0947\}$.

The weights between the hidden nodes and the output nodes for the RBFNNs modelling the M elements are

Table 1. Physical properties of the flexible-link and -joint manipulator.

Parameter	Symbol	Value
Link length	l	2.0 m
Outer diameter	d_o	10.0 mm
Inner diameter	d_i	5.0 mm
MI of link	I	4.6×10^{-10} m^4
Density	ρ	0.1569 kg m^{-1}
Young's modulus	E	6.9×10^{10} N m^{-2}
Rotor inertia	I_r	0.01865 kg m^2
Payload	m_p	0.2 kg
Gear ratio	G	10
Spring constant	K_s	100 Nm rad^{-1}

computed on-line by applying equation (72). The adaptation algorithm for the weights adjustment was implemented using a trapezoidal integration method with a sampling time of 1 ms. Every hidden node may have different width as explained in Section 6. However, it is reported that a uniform width is sufficient for universal approximation (Park and Sandberg 1991). Therefore, to reduce computation time here, each hidden node was assigned a uniform width fixed to a value of 10. The centres of the RBFs were distributed evenly over the operational range (Ge and Lee 1998). Choice of the number nodes used for constructing M is a compromise between minimizing computational speed and maximizing the RBFNN performance. A greater number of nodes improves the performance but also increases the computation time required. After conducting several simulation experiments, the following parameters gave good RBFNN performance without requiring excessive computation time. The number of nodes for emulating M was chosen as 20. The gains of the singular perturbation-based NN (SPNN) controller were chosen by trial and error to minimize tracking error and the values used were: $K_n = 8.0$ and $\Gamma_{mi} = 0.2$. The initial weights were all set at random values in the range –0.05 to 0.05.

Control performances of the proposed singular perturbation controllers along with the modified computed torque control applied to this manipulator are given in figures 6–11.

Figure 6 shows that the MODCT has the maximum amplitude of tracking error whilst the error in case of SPNN is the minimum and converges with the least time. Joint deflection trajectories obtained with the application of the three controllers are shown in figure 7. In the case of MODCT control, the deflection has the highest value among the three controllers while the SPNN yielded the lowest. Moreover, joint deflection

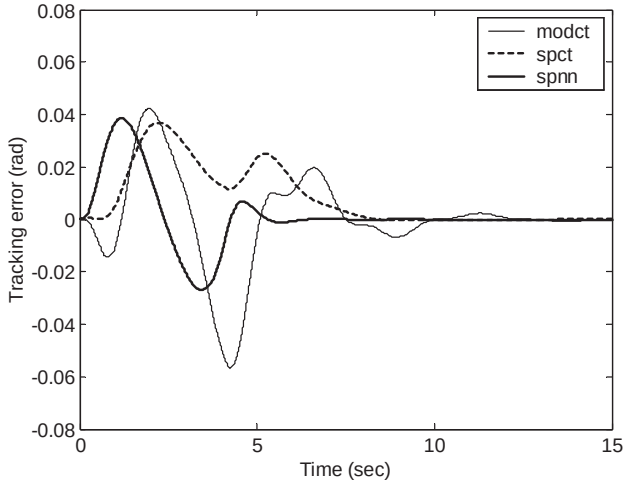

Figure 6. Comparison of tracking errors.

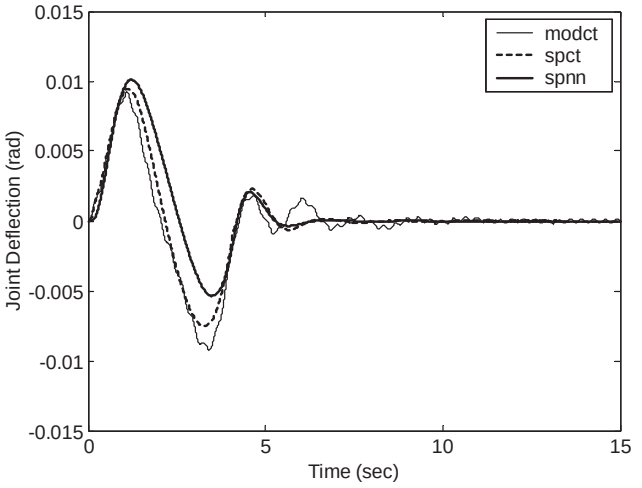

Figure 7. Joint deflection trajectories.

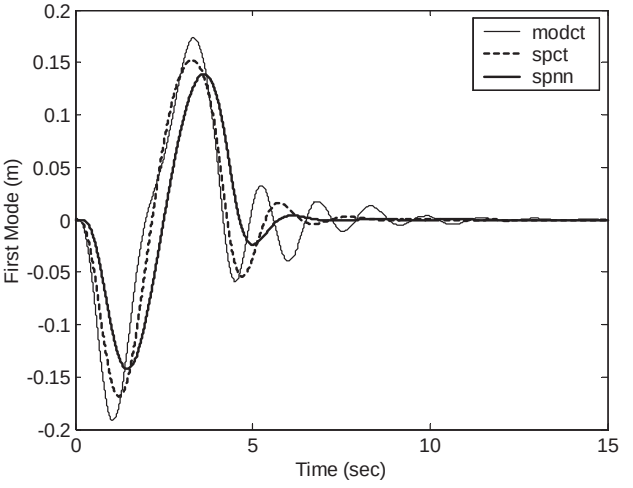

Figure 8. Time variation of the first modal vibration.

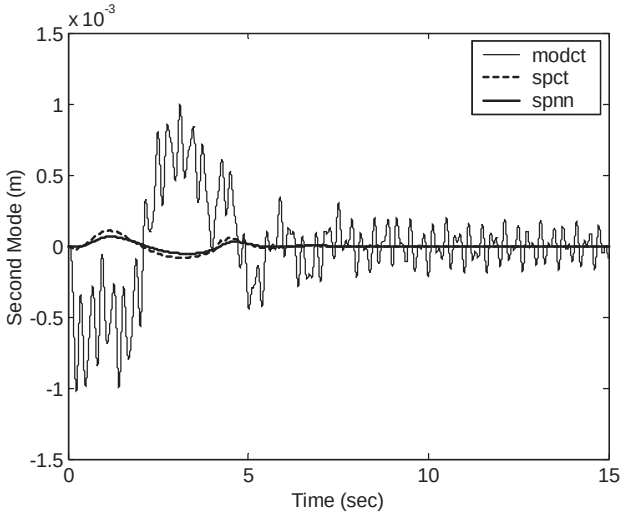

Figure 9. Time variation of the second mode of vibration.

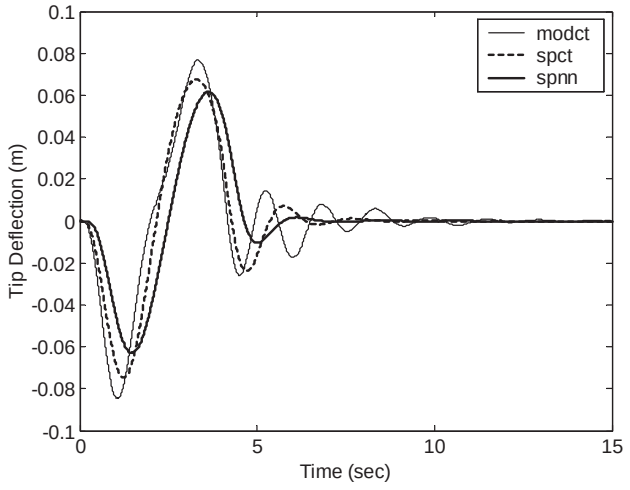

Figure 10. Tip deflection trajectories.

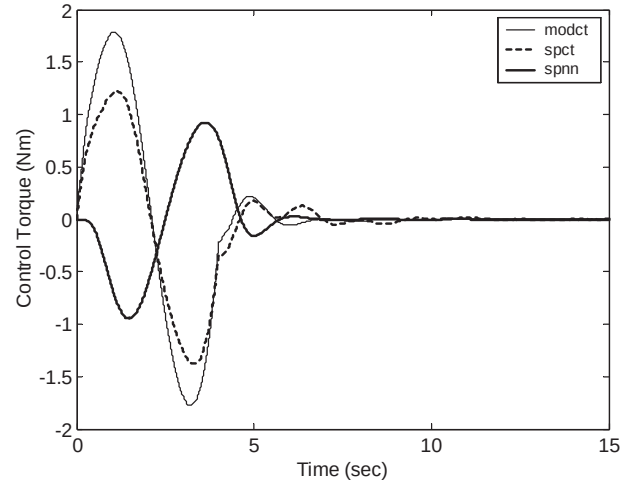

Figure 11. Control torque profiles.

with SPNN and SPCT are damped out faster compared with MODCT. Figures 8 and 9 show that the amplitudes of the first modes of vibration for the link are bigger than the corresponding second modes for both the controllers. In addition, the first and second modes have the largest amplitudes in the case of MODCT followed by SPCT and SPNN. The proposed SPNN also takes least time to damp out these modal vibrations. As both the modes of vibration have been excited in the case MODCT, therefore the corresponding tip deflection is greater compared with both SPCT and SPNN (figure 10). However, with the application of the proposed singular perturbation controllers, both the modes of vibrations of the link are suppressed very quickly as compared with MODCT. Figure 11 compares the profiles of control torques generated for the manipulator with these control schemes. The maximum values of joint torques are 1.76, 1.24 and 0.87 Nm, respectively, for MODCT, SPCT and SPNN. The control signals generated with the three schemes are shown in figure 11. The control signals approach zero as the link position tracking error and the tip/joint deflections approach zero. Control torque requirement with MODCT is more than both the SPCT and SPNN.

8. Conclusion

The dynamic equations of a single-link flexible manipulator with elastic joint has been derived by using the Euler–Lagrange principle and the assumed modes discritization technique, which can be extended to a multilink flexible manipulator with suitable appendages. The advantage of the singular perturbation approach is that the amount of on-line computation is reduced, and it is very useful for multilink robots because the product terms involving $(\theta, \dot{\theta}, q, \dot{q})$ do not appear in the real-time control torque computation. Controlling the complex flexible link and flexible joint manipulator becomes simpler through the use of the proposed singular perturbation approach in respect of difficulties such as under actuation. Good tracking performance and active damping of the link and joint deflections are achieved by the proposed singular perturbation controller schemes. Furthermore, the use of neural networks for deriving control action for the slow dynamics has provided an improved performance compared with the singular perturbation control that uses computed torque control technique due to the robustness of the NNs in the face of model uncertainty.

Note that a two-time-scale singularly perturbed model of a manipulator with both flexible links and joints have been derived using a single perturbation parameter in this paper. Similar development can easily be obtained by considering two perturbation parameters corresponding to different ratios of the link and joint stiffness (case I: $K_w > K_s$, case II: $K_w < K_s$ and K_w and K_s are of same order). The paper has dealt with singular perturbation modelling assuming a full order dynamic model is available. However, the results can be further extended to non-model-based control (Ge *et al.* 2001b).

Acknowledgement

The authors thank the anonymous reviewers for their careful reading and suggestions to improve the quality of the paper.

References

Aoustin, Y., and Chevallereau, C., 1993, The singular perturbation control of a two-flexible link robot. In *Proceedings of the IEEE International Conference on Robotics and Automation*, Atlanta, GA, pp. 737–742.

Aoustin, Y., Chevallereau, C., Glumineau, A., and Moog, C. H., 1994, Experimental results for the end-effector control of a single

flexible robotic arm. *IEEE Transactions of Control System Technology*, **2,** 371–380.

BAYO, E., 1987, A finite element approach to control the end-point motion of a single-link flexible robot. *Journal of Robotic Systems*, **4,** 63–75.

CETINKUNT, S., and YU, W. L., 1991, Closed-loop behaviour of feedback-controlled flexible arm: a comparative study. *International Journal of Robotics Research*, **10,** 263–275.

CHAPNIK, B. V., HELPER, G. R., and APLEVICH, J. D., 1991, Modelling impact on a one-link flexible robotic arm. *IEEE Transactions of Robotics and Automation*, **7,** 479–488.

EVERETT, L. J., 1989, An extension of Kanes method for deriving equations of flexible manipulators. In *Proceedings of the IEEE Conference on Robotics and Automation*, pp. 391–398.

GE, S. S., 1996, Adaptive controller design for flexible joint manipulators. *Automatica*, **32,** 273–278.

GE, S. S., LEE, T. H., and HARRIS, C. J., 1998, *Adaptive Neural Network Control of Robotic Manipulators* (London: World Scientific).

GE, S. S., LEE, T. H., and WANG, Z. P., 2001a, Adaptive neural network control for smart materials robots using singular perturbation technique. *Asian Journal of Control*, **3,** 143–155.

GE, S. S., LEE, T. H., and WANG, Z. P., 2001b, Model-free regulation of multi-link flexible smart materials robots. *IEEE/ASME Transactions on Mechatronics*, **6,** 346–351.

GE, S. S., and POSTLETHWAITE, I., 1995, Adaptive neural network controller design for flexible joint robots using singular perturbation technique. *Transactions of the Institute of Measurement and Control*, **17,** 120–131.

GENIELE, H., PATEL, R. V., and KHORASANI, K., 1997, End-point control of a single link flexible manipulator: theory and experiments. *IEEE Transactions on Control Systems Technology*, **5,** 556–560.

GOGATE, S., and LIN, Y. J., 1993, Formulation and control of robots with link and joint flexibility. *Robotica*, **11,** 273–282.

HAYKINS, S., 1998, *Neural Networks, A Comprehensive Foundation* (Upper Saddle: Prentice-Hall).

KHORASANI, K., 1992, Adaptive control of flexible joint-robots. *IEEE Transactions on Robotics and Automation*, **8,** 251–267.

KOKOTOVIC, P. V., 1984, Applications of singular perturbation techniques to control problems. *SIAM Review*, **26,** 501–550.

LEWIS, F. L., LIU, K., and YESILDIREK, A., 1995, Neural net robot controller with guaranteed tracking performance. *IEEE Transactions on Neural Networks*, **6,** 703–715.

LI, Y., BAOJIAN, T., ZHIXIA, S., and YOUFANG, L., 2000, Experimental study for trajectory tracking of a two-link flexible manipulator. *International Journal of Systems Science*, **31,** 3–9.

MEIROVITCH, L., 1986, *Elements of Vibration Analysis* (Singapore: McGraw-Hill).

MOALLEM, M., KHORASANI, K., and PATEL, R. V., 1997, An integral manifold approach for tip-position tracking of flexible multi-link manipulators. *IEEE Transactions on Robotics and Automation*, **13,** 823–865.

PARK, J., and SANDBERG, I. W., 1991, Universal approximation using radial-basis-function networks. *Neural Computation*, **3,** 246–257.

SAKSENA, V. R., O'REILIY, J., and KOKOTOVIC, P. V., 1984, Singular perturbations and time-scale methods in control theory: survey. *Automatica*, **2,** 273–293.

SANNER, R. M., and SLOTINE, J. E., 1992, Gaussian networks for direct adaptive control. *IEEE Transactions on Neural Networks*, **3,** 837–863.

SICILIANO, B., and BOOK, W. J., 1988, A singular perturbation approach to control of lightweight flexible manipulators. *International Journal of Robotics Research*, **7,** 79–90.

SICILIANO, B., PRASAD, J. V. R., and CALISE, A. J., 1992, Output feedback two-time scale control of multi-link flexible arms. *Transactions of the ASME Journal of Dynamic Systems, Measurement and Control*, **114,** 7–77.

SPONG, M. W., 1987, Modelling and control of elastic joint robots. *Transactions of the ASME Journal of Dynamic Systems, Measurement and Control*, **109,** 310–319.

SPONG, M. W., 1989, Adaptive control of flexible joint robots. *Systems and Control Letters*, **13,** 273–278.

USORO, P. B., NANDIRA, R., and MAHIL, S. S., 1986, A finite element/Lagrange approach to modelling lightweight manipulators. *Transactions of the ASME Journal of Dynamic Systems, Measurement and Control*, **108,** 198–205.

VANDERGRIFT, M. W., LEWIS, F. L., and ZHU, S. Q., 1994, Flexible-link robot arm control by feedback linearization/singular perturbation approach. *Journal of Robotic Systems*, **11,** 591–603.

YANG, G. B., and DONATH, M., 1988, Dynamic modelling of a one link robot manipulator with both structural and joint flexibility. In *Proceedings of the IEEE Conference on Robotics and Automation*, pp. 476–481.

YUAN, K., and LIN, L. C., 1991, Motor based control of manipulators with flexible joints and links. In *Proceedings of the IEEE Conference on Robotics and Automation*, pp. 1809–1814.